HHS Public Access

Author manuscript

Biomech Model Mechanobiol. Author manuscript; available in PMC 2018 February 01.

Published in final edited form as:

Biomech Model Mechanobiol. 2017 February ; 16(1): 213–225. doi:10.1007/s10237-016-0811-4.

Glycosaminoglycans Contribute to Extracellular Matrix Fiber Recruitment and Arterial Wall Mechanics

Jeffrey M. Mattson[†], **Raphaël Turcotte**[‡,§], and **Yanhang Zhang**[†,‡,*]

[†]Department of Mechanical Engineering, Boston University, Boston, Massachusetts, USA

[‡]Department of Biomedical Engineering, Boston University, Boston, Massachusetts, USA

[§]Center for Systems Biology, Advanced Microscopy Program, Wellman Center for Photomedicine, Massachusetts General Hospital, Harvard Medical School, Boston, Massachusetts, USA

Abstract

Elastic and collagen fibers are well-known to be the major load-bearing extracellular matrix (ECM) components of the arterial wall. Studies of the structural components and mechanics of arterial ECM generally focus on elastin and collagen fibers, and glycosaminoglycans (GAGs) are often neglected. Although GAGs represent only a small component of the vessel wall ECM, they are considerably important because of their diverse functionality and their role in pathological processes. The goal of this study was to study the mechanical and structural contributions of GAGs to the arterial wall. Biaxial tensile testing was paired with multiphoton microscopic imaging of elastic and collagen fibers in order to establish the structure-function relationships of porcine thoracic aorta before and after enzymatic GAG removal. Removal of GAGs results in an earlier transition point of the nonlinear stress-strain curves ($p<0.05$). However, stiffness was not significantly different after GAG removal treatment, indicating earlier but not absolute stiffening. Multiphoton microscopy showed that when GAGs are removed, the adventitial collagen fibers are straighter, and both elastin and collagen fibers are recruited at lower levels of strain, in agreement with the mechanical change. The amount of stress relaxation also decreased in GAG depleted arteries ($p<0.05$). These findings suggest that the interaction between GAGs and other ECM constituents plays an important role in the mechanics of the arterial wall, and GAGs should be considered in addition to elastic and collagen fibers when studying arterial function.

Keywords

Glycosaminoglycan; proteoglycan; collagen; elastin; multiphoton microscopy; biaxial tensile testing; fiber recruitment; extracellular matrix

[*]Correspondence: yanhang@bu.edu, T: (617) 358-4406, F: (617) 353-5866.

7. Conflict of interest

The authors confirm that there are no conflicts of interest associated with this publication.

1. INTRODUCTION

The wall of an artery contains elastic and collagen fibers, as well as ground substance including glycosaminoglycans (GAGs). Together they compose the extracellular matrix (ECM) interspersed among organized layers of cells. Elastic fibers are essential to accommodate deformations encountered during physiological function of arteries, which undergo repeated cycles of extension and recoil, while the extensibility of the tissue are associated with the collagen fibers. Studies of the structural components and mechanics of arterial ECM generally focus on elastic and collagen fibers while GAGs are often neglected, most likely because of their relatively low content (2–5% by dry weight) in arterial tissue (Wight 1980). Recent studies showed that GAGs influence viscoelasticity as well as residual stress, which plays an important role in arterial homeostasis (Wight 1980; Azeloglu et al. 2008). GAGs have also been hypothesized to contribute to mechanosensing, which can be disrupted under pathological conditions that can lead to wall delamination (Roccabianca et al. 2014a; Roccabianca et al. 2014b). Additionally, the mechanical interactions of GAGs with elastic and collagen fibers are not fully understood. The swelling pressure of inflated GAGs imposes tensile loading of the fiber network, which in turn entangles/restrains the GAGs within the ECM, as well as provide shear stiffness to the ECM and help maintain ECM organization (Maroudas 1976; Zhu et al. 1996; Takahashi et al. 2014). Taken together the above observations call for a more in depth understanding of GAGs contribution to aorta mechanics and cardiovascular diseases such as diabetes, atherosclerosis, aneurysm, and hypertension for which altered ECM is a hallmark.

GAGs are long, unbranched chains of repeating disaccharide units that are classified into four groups: chondroitin sulfate/dermatan sulfate (previously chondroitin sulfate B), heparan sulfate, keratan sulfate, and hyaluronan. Sulfated GAGs have a high affinity for water molecules and are negatively charged, which attract cations and thus water to maintain osmotic equilibrium as well as repulse each other to serve as a mechanism for resisting compression and shear (Cavalcante et al. 2005). GAGs bound to a core protein form proteoglycans (PGs), which aggregate by attaching to hyaluronan, the only non-sulfated GAG.

PGs are found in different locations in the arterial wall, which may indicate differences in function of each PG family that is classified by the types of GAGs that comprise them (Camejo et al. 1998; Dingemans et al. 2000). The majority of PGs are believed to reside in the media and can associate with elastin, collagen, cells, or be found in interstitial space (Halper 2014). Of the total amount of GAGs in the thoracic aorta of various species, chondroitin sulfate is the most abundant at 40–56%, with the remainder being 4–30% dermatan sulfate, 9–32% heparan sulfate, and 4–24% hyaluronan (Aikawa et al. 1984). Chondroitin/dermatan sulfate forms collagen fiber-associated, non-aggregating decorin and biglycan PGs, as well as versican, a large interstitial PG that aggregates along hyaluronan and can interact with elastin (Humphrey 2013). Heparan sulfate is found on perlecan, a cell-associated PG that also aggregates along hyaluronan and interacts with the fibrillin of elastic fibers (Hayes et al. 2011).

It has long been speculated that the elastic fibers of healthy central arteries contribute at lower levels of strain, whereas collagen fibers are recruited at higher levels to create nonlinear passive mechanical behavior (Burton 1954). Our recent studies using multiphoton microscopy demonstrate an interesting sequential engagement of elastic and collagen fibers in response to mechanical loading (Chow et al. 2014; Turcotte et al. 2016). Such intrinsic interrelation between elastic and collagen fibers is essential for an artery to function normally. The contribution of GAGs to arterial mechanics is only recently gaining attention (Roccabianca et al. 2014b). Due to the unique presence and properties of GAGs in the arterial wall, they may play a role in engaging the ECM fibers in the arterial wall and thus indirectly affect its biomechanical function.

To understand the role of GAGs in the passive mechanical behavior of thoracic aorta, biaxial tensile and stress relaxation tests were performed to characterize the elastic and viscoelastic properties of untreated tissue and treated tissue with GAGs enzymatically removed. Multiphoton microscopy was performed to study the structural organization of elastic and collagen fibers in the arterial wall when GAGs are absent. Mechanical testing was paired with multiphoton microscopy to establish insightful structure-function understandings.

2. MATERIALS AND METHODS

2.1 Sample Preparation

Descending porcine thoracic aortas were obtained (12–24 months, 160–200 pounds) from a local abattoir and cleaned of loose connective/fatty tissue. Approximately 20 mm sized square samples (n=6, from 3 aorta with 2 cuts each) were cut so that one edge is parallel to the longitudinal direction and the other edge is parallel to the circumferential direction of the artery. Untreated samples were mechanically tested within 12 hours after harvesting.

2.2 Enzymatic GAG Removal Treatment

To enzymatically remove GAGs in arterial tissue, a protocol adapted from Lovekamp *et al.* (Lovekamp et al. 2006) was used by adding heparinase to the treatment. Briefly, samples were treated in 100 mM ammonium acetate buffer, pH 7.0, 2–5 U/mL hyaluronidase, 0.025 U/mL chondroitinase ABC, 0.25 U/mL heparinase (Sigma Aldrich #H3506, C3667, H3917, St. Louis, MO) and gently agitated for 24 hours at 37°C to remove GAGs. Samples were then rinsed and mechanically tested in 150 mM phosphate buffered saline (PBS).

2.3 Histology

Histology studies were performed on tissue sections with and without GAGs removal. Samples were fixed in 10% formalin buffer (Fisher Scientific, Waltham MA) and then imbedded in paraffin. Sections of approximately 6 μm in thickness were obtained and stained with Alcian blue and Movat's pentachrome to evaluate the efficiency of the GAGs removal treatment and to inspect the structure of the remaining ECM components, respectively.

2.4 Biaxial Tensile Test

A custom designed biaxial tensile testing device was used to mechanically test the tissue samples before and after GAG removal following protocols described previously (Grashow et al. 2006; Zou and Zhang 2010; Chow et al. 2013). Briefly, tissue deformation, stretch, was measured by tracking four carbon marker dots on the tissue during a tension control protocol using a custom LabVIEW program. Samples were hooked on each edge and connected to the linear positioners with sutures. A preload of 5 ± 0.050 N/m was applied in order to straighten the sutures connecting the tissue to the device. Samples were loaded with 10 s half-cycles at 50 N/m until a consistent preconditioning response was achieved. Then the samples were subjected to a set of equibiaxial and non-equibiaxial loading conditions, 200C-400L, 300C-400L, 400C-300L, 400C-200L, and 400C-400L N/m to characterize the anisotropic mechanical behavior, where C and L represents the circumferential and longitudinal directions, respectively. The last cycle of a synchronized biaxial response was used for data analysis. Cauchy stresses were calculated as:

$$\sigma_1=\frac{F_1\lambda_1}{tL_{o2}},\sigma_2=\frac{F_2\lambda_2}{tL_{o1}}$$

where F is the applied load, λ is the stretch, L_o is the initial length, and t is the thickness of the tissue. The subscripts *1* and *2* correspond to the longitudinal and circumferential directions. True strains were calculated as:

$$\varepsilon_1=\ln\lambda_1,\varepsilon_2=\ln\lambda_2$$

where λ is the stretch.

2.5 Stress Relaxation Test

For stress relaxation tests, immediately following the cycle for 400C-400L N/m, this tension was reapplied with a 2 s rise time and held at a constant stretch for 900 s. This cyclic tension followed by stress relaxation protocol was repeated 3 to 4 times to achieve a consistent response (Zou and Zhang 2010). To quantify the effect of GAG removal on stress relaxation, normalized stress relaxation curves are obtained by normalizing to the peak stress, which was averaged with 20 adjacent data points (+/− 10 ms) to smooth any over/undershoot due to rapid loading. Percent stress relaxation is taken as the decrease in normalized value for the end of the test at 900 s.

2.6 Multiphoton Microscopy

To understand the contribution of GAGs to the structure and function of the arterial wall, and the interaction of GAGs and other ECM constituents, mechanical loading was paired with multiphoton imaging of tissue with GAGs removed following methods detailed by Chow *et al.* (Chow et al. 2014) to allow for comparison with untreated tissue. Briefly, a mode-locked Ti:sapphire laser (Maitai-HP, excitation wavelength 800 nm, 100 fs pulse width, 80 MHz repetition rate, Spectra-Physics, Santa Clara, CA) was used to generate second-harmonic generation from collagen(417/80 nm) and two-photon-excited fluorescence from elastin

(525/45 nm). Each sample was imaged with a field-of-view of 360 μm at nine locations spread over an area of 1 cm^2 to obtain the average structural properties of the sample (i.e. to minimize local artifact). Samples were imaged from both the adventitial and medial surfaces to assess adventitial collagen as well as medial collagen and elastin. Due to signal strength differences, the average power was consistently set to 40 mW for the media and 25 mW for the adventitia. The adventitial side was imaged to a depth of 60 μm, whereas the medial side was imaged to a depth of 40 μm and maximum intensity projections of the Z-stacks were made. Images were cropped from 360×360 μm^2 to 110×110 μm^2 regions with optimal fiber coverage, which were used for analysis.

All samples were imaged with the circumferential direction of the tissue aligned horizontally. Thus, fibers oriented at 0° and ±90° are in the circumferential (C) and longitudinal (L) anatomic directions of the aorta, respectively. Samples were imaged from 0 to 40% equibiaxial strain in 5% increments. These images were then used in the analysis of fiber straightening and recruitment in response to mechanical loading. To examine the effect of GAG removal on fiber mobility/reorientation, treated samples were imaged at equal and non-equibiaxial deformation of 30C-30L, 15C-30L, and 30C-15L where the numbers represent grip-to-grip percentile engineering strain. Samples took 2–3 minutes to image for each side at each strain level.

2.7 Imaging analysis

Fiber orientation, frequency of fiber angle, was determined from two-dimensional fast Fourier transform analysis using the Directionality plug-in in FIJI (fiji.sc/Fiji, Ashburn, VA) following the developer's instructions. The main calculation of the directionality plugin is a 2D fast Fourier transform. The fiber orientation is thus determined in the spatial frequency space. The quantification involves neither the absolute number of fibers, nor the planar area of fibers. Instead, it is the normalized power spectral density along the radial direction, taken at 2° increment, which represent the amount of fibers. To quantify fiber reorientation, fiber ratio was quantified by calculating the ratio of circumferential (0°±20°) to longitudinal (±90°±20°) fibers at each level of stretch. Fiber mobility was then determined by dividing the fiber ratio of unequal stretch by the ratio of equal stretch. Comparisons were made between treated samples and our previously published untreated samples published (Chow et al. 2014).

Adventitial collagen fiber waviness was quantified with NeuronJ (imagescience.org/meijering/software/neuronj) by measuring the end-to-end distance (L_o) and total fiber length (L_f), to define a straightness parameter:

$$P_s = L_0 / L_f$$

which is equal to 1 for a straight line (Chow et al. 2014).

Measuring the straightness parameter requires manually tracing the profile of individual fibers from raw images. This cannot be done in the media because both collagen and elastin fibers form complex networks in which individual fibers are not easily discerned. To

overcome this limitation, fractal analysis was established in previous work as a broad measure of fiber recruitment (Chow et al. 2014). The fully automated nature of fractal analysis makes it suitable for use in the intricate collagen and elastin medial networks. The straightness parameter for the adventitial layer is presented as a validation and to reinforce conclusions made using the fractal analysis. The larger fibers in the adventitia form larger bundles, thus ensuring robustness of the manual tracing. In this case, it is thus possible to evaluate the straightness parameter with minimal bias. Fractal analysis can be summarized as follows. A box counting protocol of ImageJ gives a fractal dimension that is a measure of self-similarity of an image. The fractal number, D, can be approximated as:

$$D \approx \log(N_r)/\log(r)$$

where r is the box size and N_r is the number of boxes required to cover the image with the box size of r. To limit sensitivity of variation between samples, results are expressed as the absolute value of $(D - D_o)/D_o$, where D and D_o are the average fractal number for the deformed and undeformed state, respectively.

2.8 Statistical Analysis

Experimental data are summarized and plotted with mean ± standard error of the mean. Two-tailed paired t-tests were used for analysis with $p<0.05$ considered as statistically significant.

3. RESULTS

We first validated the efficiency of the GAG removal treatment and its impact on ECM fiber integrity. Histology images show effective GAG removal and that the collagen and elastic fibers remain intact (Figs. 1 and 2). Alcian blue stains GAGs in blue, which were observed throughout the thickness of the untreated tissue (Fig. 1a). Effective GAG removal was confirmed by the absence of blue staining in the treated tissue (Fig. 1b). Movat's stain also results in GAGs appearing blue in untreated tissue, as well as staining elastic fibers in black, collagen fibers in yellow, and smooth muscle in red (Fig. 2a). The fibers remain intact after treatment, however more empty spaces where the GAGs have been removed are observed in the treated tissue (5.1% for treated vs. 0.8% for untreated, Fig. 2). Here empty spaces were quantified in the Movat's histology stain images of the medial layer using ImageJ by minimizing the brightness, then making the image binary and using the "analyze particles" feature (Tan and Sanderson 2014). Note that empty spaces are not quantified for the adventitial layer due to the more prevalent white spaces in the tissue.

We then evaluated the impact of GAG removal on the biomechanical function of arteries. Averaged stress-strain curves of samples before and after removing GAGs are shown in Fig. 3a. To quantify the changes in mechanical properties due to GAG removal, initial and stiff slopes were determined by linear fit to the regions of stress-strain curves from 0–20 kPa and 180–200 kPa, respectively. The low stress region was chosen to include as many data points as possible to capture the stiffness at the initial toe region, while remaining in a linear region. The high stress region was chosen such that the adventitial collagen fibers are

recruited. Transition stress/strain was then calculated as the intersection of the bilinear curve fit to the initial and stiff regions of the stress-strain curves (Chow et al. 2011). For treated samples, the transition points of the circumferential ($p=0.04$) and longitudinal ($p=0.002$) directions are at significantly lower strain measurements, indicating earlier stiffening behavior of the arterial wall (Fig. 3b). However, the initial and stiff slopes for each direction are not significantly different after treatment (Fig. 4, all $p>0.1$), suggesting GAG removal results in earlier stiffening, but the integrity of the remaining elastin and collagen was not compromised.

Non-equibiaxial testing showed similar results to equibiaxial testing, with treated samples stiffening at lower strains than untreated samples (Figs. 5a, b). To examine the effect of GAG removal on mechanical coupling between material axes, axial cross-coupling was quantified by dividing the peak true strain for each non-equibiaxial tension condition (ε) by the peak true strain for the equibiaxial tension condition (ε_{eq}) for that sample (Sacks and Chuong 1998), since non-equibiaxial tension loading would result in a larger stretch in the direction with higher tension. It appears that after GAG removal, there were minimal changes to axial cross-coupling (Fig. 5c), which suggests that GAG removal does not affect fiber mobility under non-equibiaxial loading.

Stress relaxation tests were performed to examine the contribution of GAGs to the viscoelastic behavior of arteries (Fig. 6a). Removing GAGs significantly reduce the percent stress relaxation from 8.766±0.007% to 7.140±0.005% ($p=0.01$) and 9.900±0.014% to 7.830±0.008% ($p=0.03$) in the longitudinal and circumferential directions, respectively. The rate of relaxation was obtained from the semi-log plot (all $R^2=0.99$, Fig. 6b). The first time point used was at 20 s, ten times larger than the rise time to prevent transient effects from a loading that it not truly a step function (Provenzano et al. 2001). GAG depletion significantly reduced the rate of relaxation in the longitudinal direction from 0.89±0.0064 to 0.65±0.042 ($p=0.04$) with the same trend in the circumferential direction from 0.99±0.12 to 0.71±0.031 ($p=0.05$).

Multiphoton imaging enabled us to visualize the structural changes in elastin, medial collagen and adventitial collagen fiber networks. GAGs are closely associated with elastin and collagen fibers, thus removal of GAGs may affect the orientation/recruitment of these two major ECM components, which dominate the mechanical function of the arterial wall. Large bundles of collagen fibers were observed in the adventitial layer (Fig. 7). The medial collagen fibers appeared as a network of rather finer fibers. Upon mechanical stretching, both adventitial and medial collagen fibers became noticeably straightened. Minimal changes in elastin fiber network with mechanical stretch were observed.

The fiber orientation was plotted from 0% to 40% equibiaxial strain in 10% increments (Fig. 8). The appearance of multiple peaks in adventitial collagen corresponds with the existence of fiber bundles/families in the adventitial layer (Fig. 8a). These peaks become more evident with fiber straightening due to increased biaxial strain. A more detailed explanation on this interpretation and confounding factors can be found in the study by Chow et al. (Chow et al., 2014). The medial collagen fibers are predominantly circumferentially oriented and becomes

more so with increased strain (Fig. 8b). Medial elastin shows minimal changes in fiber distribution with mechanical loading (Fig. 8c).

To quantify fiber reorientation/mobility, fiber ratio was quantified by calculating the ratio of circumferential (0°±20°) to longitudinal (±90°±20°) fibers at each level of stretch. Fiber mobility was then determined by dividing the fiber ratio of unequal stretch by the ratio of equal stretch. Comparisons were made between treated samples and previously published untreated samples (Chow et al. 2014). The fiber mobility analysis suggests that both untreated and treated tissue shows more fiber mobility towards the circumferential than longitudinal direction for adventitial and medial collagen fiber networks, as demonstrated in Figs. 9a and 9b. GAG removal results in minimal changes to fiber reorientation under non-equibiaxial deformation ($p>0.2$).

Waviness of adventitial collagen fibers was quantified with the straightness parameter (Fig. 10a). At 0% strain, the straightness parameter for adventitial collagen fibers of tissue with GAGs removed ($P_s=0.920\pm0.005$) was significantly higher than for untreated tissue ($P_s=0.855\pm0.017$) from Chow *et al.* (Chow et al. 2014). While delayed collagen fiber engagement behavior, i.e., fibers do not show significant straightening until around 20% strain, was observed in the adventitial collagen from untreated tissue, this behavior is absent from the treated tissue. With GAG removal, the initially straightened collagen fibers show a less evident but continuous straightening process with increased mechanical strain.

Fractal analysis further revealed that the treated samples show smaller changes in fiber recruitment (Figs. 10b–d). These results are consistent with the finding that the ECM fibers appear to be straighter and are engaged earlier than the untreated tissue. For the untreated tissue, our earlier study (Chow et al. 2014) reported an interesting sequential elastin and collagen fiber recruitment, which suggests an intrinsic structural and functional interrelation among ECM constituents. Briefly, elastin is recruited early and then plateaus at about 20% strain, medial collagen is continuously recruited, and adventitial collagen has a delayed recruitment around 20% strain (Chow et al. 2014). With GAG removal, however, in general such sequential trend in fiber recruitment disappears, and all fibers are recruited early and have small changes afterward (Fig. 10).

4. DISCUSSION

GAGs/PGs serve many functions in development, maintenance, and repair of a variety of tissues (Couchman and Pataki 2012; Halper 2014). Furthermore, GAG content begins decreasing with age after the first 40 years of life, as well as with pathologies such as osteoarthritis (Maroudas 1976; Tovar et al. 1998). An increase in GAG depleting enzymes such as those used in this study are also noted in conditions such as hyperglycemia and hyperlipidemia that are prevalent in diabetes and atherosclerosis (Baker et al. 2009; Wang et al. 2009; Baker et al. 2010). Building upon our prior research on ECM mechanics, the present study integrates biomechanical characterization and multiphoton imaging to explore how GAGs contribute to the structural and biomechanical integrity of arteries. Biaxial tensile testing allows full characterization of the anisotropic mechanical behavior of the tissue under well-defined loading conditions, which is essential in order to capture changes in mechanical

function with GAG removal. Multiphoton microscopy provides microstructural assessment of elastic and collagen fibers, and offers insightful explanations on the functional and regulatory significance of GAGs in the arterial wall. Overall, our study suggests that despite the relatively low mass fraction of GAGs in arterial tissue, GAGs play an important role in contributing to the structural and mechanical properties of the arterial wall.

The finding of decreased stress relaxation after removing GAGs suggests that GAGs contribute to the viscoelastic behavior of arteries. In cartilage, GAGs attract water and upon tissue deformation, fluid motion flows relative to the collagen-GAG solid phase, creating friction and shear (Mow et al. 1980). This effect, combined with the osmotic swelling due to the ionic charge of GAGs, was assumed to contribute to the viscoelastic and tensile behavior of cartilage based on mixture theory (Lai et al. 1991; Ateshian et al. 2009). More recently, a similar concept was applied to study the GAGs in arteries (Azeloglu et al. 2008). However, in addition to collagen, arteries contain elastin and cells as two other main structural components, so there may be additional interaction effects between these components and GAGs. GAGs not only cross-link collagen fibrils, but also anchor to the cell surface such as hyaluronan anchoring to receptors CD44 or RHAMM (Evanko et al. 2007). Also, the protein cores of biglycan and decorin PGs each have similar yet distinct binding sites on the tropoelastin of elastic fibers (Reinboth et al. 2002).

GAGs have been found to affect the mechanics of other soft tissue, such as tendon, lung, heart valve, and eye, though results are tissue-specific and sometimes contradictory. For example, GAG depletion increased the stress relaxation response of tendon fascicles, perhaps from water movement or collagen sliding (Legerlotz et al. 2013). Indeed, PGs may reduce collagen sliding by forming interfibrillar bridges (Scott 2003). Alternatively, PGs could promote collagen sliding in tendon by isolating neighboring collagen fibrils (Rigozzi et al. 2013). Additionally, controversial results were obtained in studying the viscoelastic properties of tendon after removing GAGs (Robinson et al. 2004; Fessel and Snedeker 2009). In parenchymal lung strips, removing GAGs increased hysteresivity independent of frequency from 0.1–10 Hz (Jamal et al. 2001). On the other hand, removing GAGs in aortic heart valves reduced hysteresis (Eckert et al. 2013) and stress relaxation (Borghi et al. 2013). Hysteresis was also decreased in the eye sclera after GAG depletion, along with decreased low-pressure stiffness, but increased high-pressure stiffness and transition point (Murienne et al. 2015). In the present study, removing GAGs decreased stress relaxation and decreased transition point in porcine thoracic aorta. These tissue-specific differences serve as a reminder of the variety of functions and mechanical conditions that the same ECM components serve among different tissues.

GAG removal also results in straighter adventitial collagen fibers even when unloaded (Figs. 7 and 10a). Previous histology studies suggest that GAGs fit within wavy collagen fibers perpendicular to the local fiber direction, similar to a laterally supported Euler column (Bellini et al. 2014). Such interactions may contribute to the entanglement of fibers, and provide support to fibers. Moreover GAGs can delay fiber engagement in the direction of mechanical loading. Collagen and elastin fibers are after all, the main load bearing components of arterial tissue experiencing cyclic tension in vivo (Wagenseil and Mecham 2009). As a result of GAG removal, these fibers can engage earlier in response to

mechanical loading. Our earlier study reported a sequential engagement of elastin and collagen fibers in response to mechanical loading. Specifically, the adventitial collagen shows a delayed fiber engagement at about 20% of equibiaxial tissue stretch, while the medial collagen and elastin fibers are engaged immediately upon mechanical loading (Chow et al. 2014). Interestingly, our mechanical study combining transition point (Fig. 3b) with axial cross-coupling analysis (Fig. 5c) together with imaging analysis (Fig. 10) indicates earlier fiber recruitment due to fiber straightening, but minimal changes to fiber mobility after GAG removal. Such well-defined structural roles of ECM components are crucial for arteries to maintain normal mechanobiological function. The present study demonstrates that the straighter fibers after GAG removal may allow the tension-resisting adventitial collagen fibers to engage at lower levels of mechanical stretch.

After GAG removal, the transition point was significantly lower (Fig. 3b). This suggests that GAGs actually play an important structural and mechanical role in tissue mechanics. Results of multiphoton imaging show that after removing GAGs, medial and adventitial collagen fibers are straighter and recruited at lower levels of strain (Fig. 10). Thus, the imaging establishes a structure-function relationship supporting the finding of lower transition point from straighter fibers that are recruited at lower levels of strain. The adventitial collagen fibers are straighter even in the unloaded state from straightness parameter analysis (Fig. 10a). In fact, removing GAGs has a similar effect on the waviness of adventitial collagen fibers to applying between 20% (P_s=0.903) and 25% (P_s=0.941) strain to untreated tissue (Chow et al. 2014). A possible explanation is that GAGs inflated from the repulsive charges and swelling pressure may contribute to collagen fiber waviness, so removing GAGs would allow the collagen fibers to be straighter.

Collagen fiber waviness has also been attributed to tensile elastin applying a compressive load on the collagen fibers (Zeinali-Davarani et al. 2013; Chow et al. 2014). Removing elastic fibers with elastase treatment results in straighter collagen fibers, a similar outcome as with mechanical stretching. Zeller and Skalak (1998) also found that the perimeter of arterial rings increased with elastase, interpreted as the removal of tensile elastin that was compressing the tissue resulting in longer tissue (Zeller and Skalak 1998). Additionally, Lillie and Gosline (2006) found that contour length of elastic lamellae decreased after releasing the residual stress, suggesting that elastin was in tension (Lillie and Gosline 2006). These experimental findings are supported by modelling that found tensile elastin was offset by compressed GAG-supported collagen and smooth muscle cells (Bellini et al. 2014). However, elastase treatment also removes GAGs, which could also contribute to the straightening of collagen fibers. Our study suggests that GAGs seem to be at least partially responsible for collagen fiber waviness since elastin remains intact after GAG removal and collagen appears to become straighter. Specifically, the inflation of GAGs could cause and fill in collagen waviness, or tensile elastin could compress collagen to make the fibers wavy and GAGs merely fill in the existing waviness.

The adventitia and media are structurally different. The collagen fiber bundles in the adventitial layer consists of primarily Type I collagen, however the media contains primarily of type III collagen. Type III collagen is thinner compared to type I fibers, and both our studies and others on second harmonic generation have shown that type III collagen

produces a much smaller signal compared to type I collagen (Chow et al., 2014). Their organization is also distinct: adventitial collagen forms bundles and medial collagen forms a more intricate network. During mechanical loading, the adventitial collagen undergoes the most visible structural changes, however the medial collagen and elastin has much less “evident” structural changes. These apparent changes translate in the magnitude of the metrics used to quantify them (SHG intensity, direct waviness measurements, and fractal analysis (Chow et al., 2014)). The magnitude of any of these metrics has no functional meaning and depends on the nature of the tissue/images. As a consequence, it is critical to avoid comparing adventitial collagen, medial collagen, and medial elastin together quantitatively. In other words, a small structural change in the medial collagen could potentially have a more significant functional impact than a large change in the adventitial collagen. However larger structural changes are more reliably quantified and arguably more sensitive. Nonetheless, it should be kept in mind that the structural changes observed in the medial collagen and elastin were also consistent with an earlier recruitment, which is the primary conclusion reported. Finally, the mechanical changes are measured on the integrated response of the tissue constituents, and the microstructural components in the arterial wall present a complex intertwined hierarchical network and different fiber components are recruited sequentially in response to mechanical loading (Chow et al., 2014). Therefore, it comes with no surprises that alteration affecting the media may lead to changes perceptible in the adventitia.

There are some limitations to studying the effect of GAGs by enzymatically removing them. Enzymatic GAG removal has been confirmed not affecting collagen stability or crosslinking in cuspal tissue, and causing no change to collagen content in articular cartilage (Bautista et al. 2016). In the present study, the remaining tissue components after GAG removal are visibly unaltered. However, the structural changes can alter attributes such as stress distributions that are not directly observable. Two-photon excited fluorescence microscopy is currently one of the most powerful techniques to image in thick and scattering tissue. Unfortunately, collagen fibers are highly scattering and birefringent, thus limiting the imaging depth to the first few layers. It should therefore be carefully noted that the structural imaging results may not reveal the average properties throughout the entire adventitia and media. GAGs has been shown to be more prevalent in the media for rat aorta (Azeloglu et al. 2008). However, our histology showed GAGs throughout the thickness for porcine aorta. The arterial ECM architecture in rodent and porcine tissue has been shown to be quite different (Fry et al. 2015). Atomic force microscopy showed changes in stiffness to both the adventitia and media after removing GAGs, which was attributed to the observation that even though GAGs are predominantly in the media, GAGs are also present in the adventitia (Beenakker et al. 2012). Since the ability of GAGs to retain water is well known, removing GAGs might affect tissue and fiber hydration that leads to altered mechanics. The effect of removing GAGs on hydration and osmotic sensitivity would be an interesting subject of future work. The depletion of GAGs also needs to be assessed quantitatively in future studies.

5. Conclusions

This study establishes several new fundamental concepts for the understanding of the role of GAGs in arterial tissue at the structural and functional levels. In summary, removal of GAGs from arterial tissue resulted in the alteration of passive mechanical properties of the tissue. Importantly, GAG removal lowered the transition point of the nonlinear stress-strain curves, which is indicative of altered mechanical function. However, the initial and stiff slopes were not significantly different, suggesting earlier stiffening via recruitment, but not absolute stiffening. Microstructural studies using multiphoton microscopy of the ECM structure revealed the presence of straighter adventitial collagen fibers, and early recruitment of both elastin and collagen fibers. Despite altering fiber recruitment via fiber straightening after removing GAGs, there were minimal changes to fiber mobility during non-equibiaxial loading. Additionally, removing GAGs reduced the per cent stress relaxation in both anatomical directions, in agreement with the idea that GAGs contribute to the viscoelastic behavior of soft tissue. Overall, this study demonstrates the importance to account for GAGs in addition to elastin and collagen when considering the contribution of ECM components to arterial mechanics.

Acknowledgments

This work was supported, in part, by a grant from National Science Foundation (CMMI 1463390) and a pre-doctoral training grant from National Institutes of Health (2T32HL007969).

References

Aikawa J, Munakata H, Isemura M, et al. Comparison of Glycosaminoglycans from Thoracic Aortas of Several Mammals. Tohoku J Exp Med. 1984; 143:107–112. [PubMed: 6464008]

Ateshian GA, Rajan V, Chahine NO, et al. Modeling the matrix of articular cartilage using a continuous fiber angular distribution predicts many observed phenomena. J Biomech Eng. 2009; 131:61003.doi: 10.1115/1.3118773

Azeloglu EU, Albro MB, Thimmappa VA, et al. Heterogeneous transmural proteoglycan distribution provides a mechanism for regulating residual stresses in the aorta. Am J Physiol - Heart Circ Physiol. 2008; 294:H1197–H1205. DOI: 10.1152/ajpheart.01027.2007 [PubMed: 18156194]

Baker AB, Chatzizisis YS, Beigel R, et al. Regulation of heparanase expression in coronary artery disease in diabetic, hyperlipidemic swine. Atherosclerosis. 2010; 213:436–442. DOI: 10.1016/j.atherosclerosis.2010.09.003 [PubMed: 20950809]

Baker AB, Groothuis A, Jonas M, et al. Heparanase Alters Arterial Structure, Mechanics, and Repair Following Endovascular Stenting in Mice. Circ Res. 2009; 104:380–387. DOI: 10.1161/CIRCRESAHA.108.180695 [PubMed: 19096032]

Bautista CA, Park HJ, Mazur CM, et al. Effects of Chondroitinase ABC-Mediated Proteoglycan Digestion on Decellularization and Recellularization of Articular Cartilage. PloS One. 2016; 11:e0158976.doi: 10.1371/journal.pone.0158976 [PubMed: 27391810]

Beenakker J-WM, Ashcroft BA, Lindeman JHN, Oosterkamp TH. Mechanical Properties of the Extracellular Matrix of the Aorta Studied by Enzymatic Treatments. Biophys J. 2012; 102:1731–1737. DOI: 10.1016/j.bpj.2012.03.041 [PubMed: 22768928]

Bellini C, Ferruzzi J, Roccabianca S, et al. A Microstructurally Motivated Model of Arterial Wall Mechanics with Mechanobiological Implications. Ann Biomed Eng. 2014; 42:488–502. DOI: 10.1007/s10439-013-0928-x [PubMed: 24197802]

Borghi A, New SEP, Chester AH, et al. Time-dependent mechanical properties of aortic valve cusps: Effect of glycosaminoglycan depletion. Acta Biomater. 2013; 9:4645–4652. DOI: 10.1016/j.actbio.2012.09.001 [PubMed: 22963848]

Burton AC. Relation of Structure to Function of the Tissues of the Wall of Blood Vessels. Physiol Rev. 1954; 34:619–642. [PubMed: 13215088]

Camejo G, Hurt-Camejo E, Wiklund O, Bondjers G. Association of apo B lipoproteins with arterial proteoglycans: Pathological significance and molecular basis. Atherosclerosis. 1998; 139:205–222. DOI: 10.1016/S0021-9150(98)00107-5 [PubMed: 9712326]

Cavalcante FSA, Ito S, Brewer K, et al. Mechanical interactions between collagen and proteoglycans: implications for the stability of lung tissue. J Appl Physiol. 2005; 98:672–679. DOI: 10.1152/japplphysiol.00619.2004 [PubMed: 15448123]

Chow M-J, Mondonedo JR, Johnson VM, Zhang Y. Progressive structural and biomechanical changes in elastin degraded aorta. Biomech Model Mechanobiol. 2013; 12:361–372. DOI: 10.1007/s10237-012-0404-9 [PubMed: 22623109]

Chow M-J, Turcotte R, Lin CP, Zhang Y. Arterial Extracellular Matrix: A Mechanobiological Study of the Contributions and Interactions of Elastin and Collagen. Biophys J. 2014; 106:2684–2692. DOI: 10.1016/j.bpj.2014.05.014 [PubMed: 24940786]

Chow M-J, Zou Y, He H, et al. Obstruction-Induced Pulmonary Vascular Remodeling. J Biomech Eng. 2011; 133:111009–111009. DOI: 10.1115/1.4005301 [PubMed: 22168741]

Couchman JR, Pataki CA. An Introduction to Proteoglycans and Their Localization. J Histochem Cytochem. 2012; 60:885–897. DOI: 10.1369/0022155412464638 [PubMed: 23019015]

Dingemans KP, Teeling P, Lagendijk JH, Becker AE. Extracellular matrix of the human aortic media: An ultrastructural histochemical and immunohistochemical study of the adult aortic media. Anat Rec. 2000; 258:1–14. DOI: 10.1002/(SICI)1097-0185(20000101)258:1<1::AID-AR1>3.0.CO;2-7 [PubMed: 10603443]

Eckert CE, Fan R, Mikulis B, et al. On the biomechanical role of glycosaminoglycans in the aortic heart valve leaflet. Acta Biomater. 2013; 9:4653–4660. DOI: 10.1016/j.actbio.2012.09.031 [PubMed: 23036945]

Evanko SP, Tammi MI, Tammi RH, Wight TN. Hyaluronan-dependent pericellular matrix. Adv Drug Deliv Rev. 2007; 59:1351–1365. DOI: 10.1016/j.addr.2007.08.008 [PubMed: 17804111]

Fessel G, Snedeker JG. Evidence against proteoglycan mediated collagen fibril load transmission and dynamic viscoelasticity in tendon. Matrix Biol. 2009; 28:503–510. DOI: 10.1016/j.matbio.2009.08.002 [PubMed: 19698786]

Fry JL, Shiraishi Y, Turcotte R, et al. Vascular Smooth Muscle Sirtuin-1 Protects Against Aortic Dissection During Angiotensin II–Induced Hypertension. J Am Heart Assoc. 2015; 4:e002384.doi: 10.1161/JAHA.115.002384 [PubMed: 26376991]

Grashow JS, Yoganathan AP, Sacks MS. Biaixal stress-stretch behavior of the mitral valve anterior leaflet at physiologic strain rates. Ann Biomed Eng. 2006; 34:315–325. DOI: 10.1007/s10439-005-9027-y [PubMed: 16450193]

Halper, J. Proteoglycans and Diseases of Soft Tissues. In: Halper, J., editor. Progress in Heritable Soft Connective Tissue Diseases. Springer; Netherlands: 2014. p. 49-58.

Hayes AJ, Lord MS, Smith SM, et al. Colocalization in vivo and association in vitro of perlecan and elastin. Histochem Cell Biol. 2011; 136:437–454. DOI: 10.1007/s00418-011-0854-7 [PubMed: 21874555]

Humphrey JD. Possible Mechanical Roles of Glycosaminoglycans in Thoracic Aortic Dissection and Associations with Dysregulated Transforming Growth Factor-Beta. J Vasc Res. 2013; 50:1–10. DOI: 10.1159/000342436 [PubMed: 23018968]

Jamal RA, Roughley PJ, Ludwig MS. Effect of glycosaminoglycan degradation on lung tissue viscoelasticity. Am J Physiol - Lung Cell Mol Physiol. 2001; 280:L306–L315. [PubMed: 11159010]

Lai WM, Hou JS, Mow VC. A triphasic theory for the swelling and deformation behaviors of articular cartilage. J Biomech Eng. 1991; 113:245–258. [PubMed: 1921350]

Legerlotz K, Riley GP, Screen HRC. GAG depletion increases the stress-relaxation response of tendon fascicles, but does not influence recovery. Acta Biomater. 2013; 9:6860–6866. DOI: 10.1016/j.actbio.2013.02.028 [PubMed: 23462553]

Lillie MA, Gosline JM. Tensile Residual Strains on the Elastic Lamellae along the Porcine Thoracic Aorta. J Vasc Res. 2006; 43:587–601. DOI: 10.1159/000096112 [PubMed: 17033196]

Lovekamp JJ, Simionescu DT, Mercuri JJ, et al. Stability and function of glycosaminoglycans in porcine bioprosthetic heart valves. Biomaterials. 2006; 27:1507–1518. DOI: 10.1016/j.biomaterials.2005.08.003 [PubMed: 16144707]

Maroudas AI. Balance between swelling pressure and collagen tension in normal and degenerate cartilage. Nature. 1976; 260:808–809. [PubMed: 1264261]

Mow VC, Kuei SC, Lai WM, Armstrong CG. Biphasic Creep and Stress Relaxation of Articular Cartilage in Compression: Theory and Experiments. J Biomech Eng. 1980; 102:73–84. DOI: 10.1115/1.3138202 [PubMed: 7382457]

Murienne BJ, Jefferys JL, Quigley HA, Nguyen TD. The effects of glycosaminoglycan degradation on the mechanical behavior of the posterior porcine sclera. Acta Biomater. 2015; 12:195–206. DOI: 10.1016/j.actbio.2014.10.033 [PubMed: 25448352]

Provenzano P, Lakes R, Keenan T, Vanderby R. Nonlinear Ligament Viscoelasticity. Ann Biomed Eng. 2001; 29:908–914. DOI: 10.1114/1.1408926 [PubMed: 11764321]

Reinboth B, Hanssen E, Cleary EG, Gibson MA. Molecular Interactions of Biglycan and Decorin with Elastic Fiber Components. J Biol Chem. 2002; 277:3950–3957. DOI: 10.1074/jbc.M109540200 [PubMed: 11723132]

Rigozzi S, Müller R, Stemmer A, Snedeker JG. Tendon glycosaminoglycan proteoglycan sidechains promote collagen fibril sliding-AFM observations at the nanoscale. J Biomech. 2013; 46:813–818. DOI: 10.1016/j.jbiomech.2012.11.017 [PubMed: 23219277]

Robinson PS, Lin TW, Reynolds PR, et al. Strain-Rate Sensitive Mechanical Properties of Tendon Fascicles From Mice With Genetically Engineered Alterations in Collagen and Decorin. J Biomech Eng. 2004; 126:252–257. DOI: 10.1115/1.1695570 [PubMed: 15179856]

Roccabianca S, Ateshian GA, Humphrey JD. Biomechanical roles of medial pooling of glycosaminoglycans in thoracic aortic dissection. Biomech Model Mechanobiol. 2014a; 13:13–25. DOI: 10.1007/s10237-013-0482-3 [PubMed: 23494585]

Roccabianca S, Bellini C, Humphrey JD. Computational modelling suggests good, bad and ugly roles of glycosaminoglycans in arterial wall mechanics and mechanobiology. J R Soc Interface. 2014b; 11:20140397–20140397. DOI: 10.1098/rsif.2014.0397 [PubMed: 24920112]

Sacks MS, Chuong CJ. Orthotropic Mechanical Properties of Chemically Treated Bovine Pericardium. Ann Biomed Eng. 1998; 26:892–902. DOI: 10.1114/1.135 [PubMed: 9779962]

Scott JE. Elasticity in extracellular matrix “shape modules” of tendon, cartilage, etc. A sliding proteoglycan-filament model. J Physiol. 2003; 553:335–343. DOI: 10.1113/jphysiol.2003.050179 [PubMed: 12923209]

Takahashi A, Majumdar A, Parameswaran H, et al. Proteoglycans Maintain Lung Stability in an Elastase-Treated Mouse Model of Emphysema. Am J Respir Cell Mol Biol. 2014; 51:26–33. DOI: 10.1165/rcmb.2013-0179OC [PubMed: 24450478]

Tan X, Sanderson MJ. Bitter tasting compounds dilate airways by inhibiting airway smooth muscle calcium oscillations and calcium sensitivity. Br J Pharmacol. 2014; 171:646–662. DOI: 10.1111/bph.12460 [PubMed: 24117140]

Tovar AM, Cesar DC, Leta GC, Mourão PA. Age-related changes in populations of aortic glycosaminoglycans: species with low affinity for plasma low-density lipoproteins, and not species with high affinity, are preferentially affected. Arterioscler Thromb Vasc Biol. 1998; 18:604–614. [PubMed: 9580254]

Turcotte R, Mattson J, WU J, et al. Second-harmonic generation in arterial collagen imaging: linking molecular order to mechanical functions using circular polarization. Biophys J. 2016; 110 accepted.

Wagenseil JE, Mecham RP. Vascular Extracellular Matrix and Arterial Mechanics. Physiol Rev. 2009; 89:957–989. DOI: 10.1152/physrev.00041.2008 [PubMed: 19584318]

Wang F, Kim MS, Puthanveetil P, et al. Endothelial heparanase secretion after acute hypoinsulinemia is regulated by glucose and fatty acid. Am J Physiol Heart Circ Physiol. 2009; 296:H1108–1116. DOI: 10.1152/ajpheart.01312.2008 [PubMed: 19218500]

Wight TN. Vessel proteoglycans and thrombogenesis. Prog Hemost Thromb. 1980; 5:1–39. [PubMed: 7422873]

Zeinali-Davarani S, Chow M-J, Turcotte R, Zhang Y. Characterization of Biaxial Mechanical Behavior of Porcine Aorta under Gradual Elastin Degradation. Ann Biomed Eng. 2013; 41:1528–1538. DOI: 10.1007/s10439-012-0733-y [PubMed: 23297000]

Zeller PJ, Skalak TC. Contribution of Individual Structural Components in Determining the Zero-Stress State in Small Arteries. J Vasc Res. 1998; 35:8–17. DOI: 10.1159/000025560 [PubMed: 9482691]

Zhu W, Iatridis JC, Hlibczuk V, et al. Determination of collagen-proteoglycan interactions in vitro. J Biomech. 1996; 29:773–783. DOI: 10.1016/0021-9290(95)00136-0 [PubMed: 9147974]

Zou Y, Zhang Y. The orthotropic viscoelastic behavior of aortic elastin. Biomech Model Mechanobiol. 2010; 10:613–625. DOI: 10.1007/s10237-010-0260-4 [PubMed: 20963623]

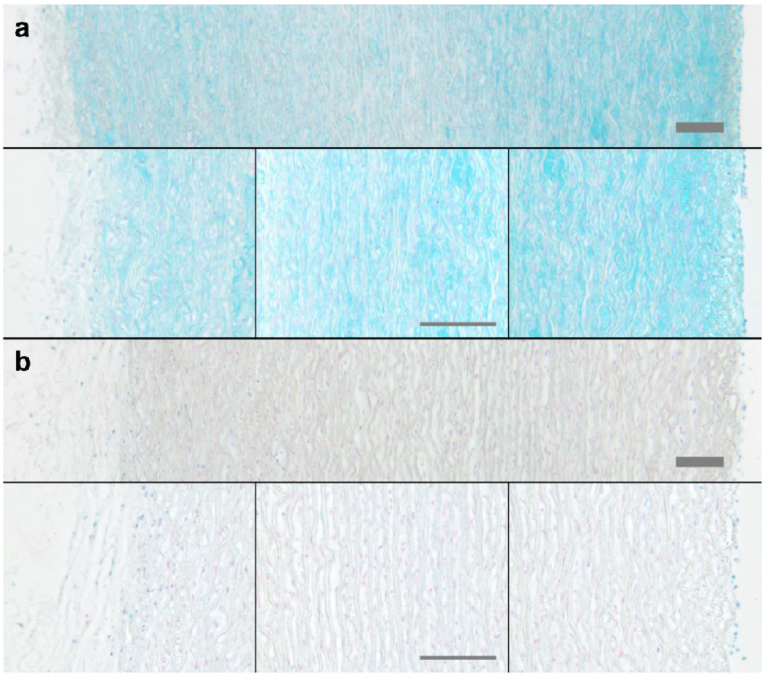

Fig. 1.

Alcian Blue stain of aorta from adventitia (left) to intima (right) for (a) untreated, and (b) treated tissue. Treated tissue shows effective enzymatic GAG removal demonstrated by the lack of blue staining. All scale bars are 100 μm.

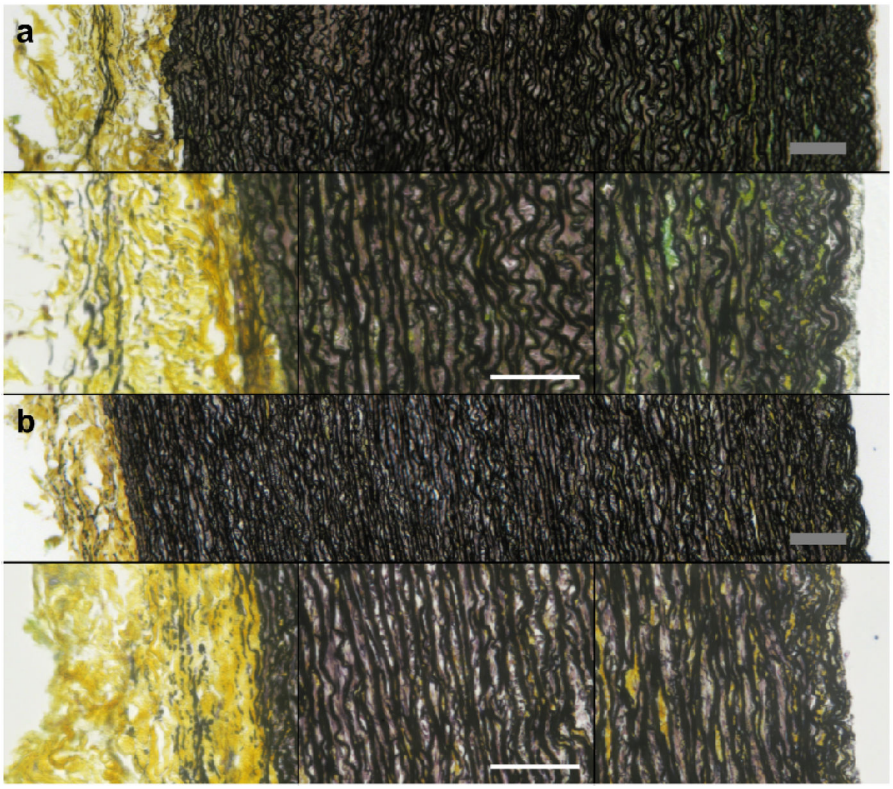

Fig. 2.

Movat's stain of aorta from adventitia (left) to intima (right) for (a) untreated, and (b) treated tissue. Collagen (yellow), elastin (black), smooth muscle (red), and GAGs (blue, untreated only). All scale bars are 100 μm.

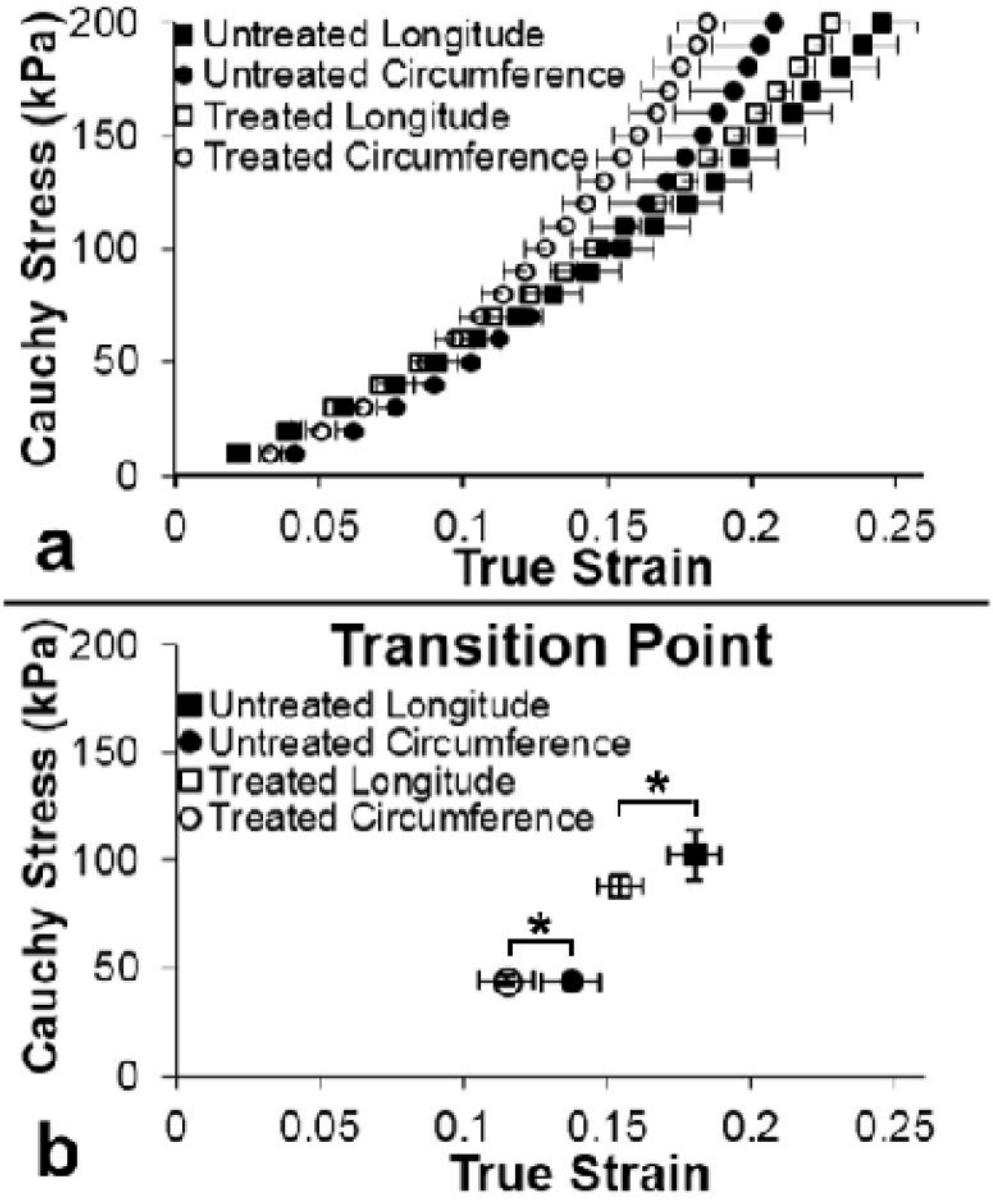

Fig. 3.

(a) Averaged stress-strain curves from equibiaxial tensile tests of aorta before and after GAG removal treatment. (b) Treated samples have transition points at significantly lower strain ($n=6$, $p<0.05$).

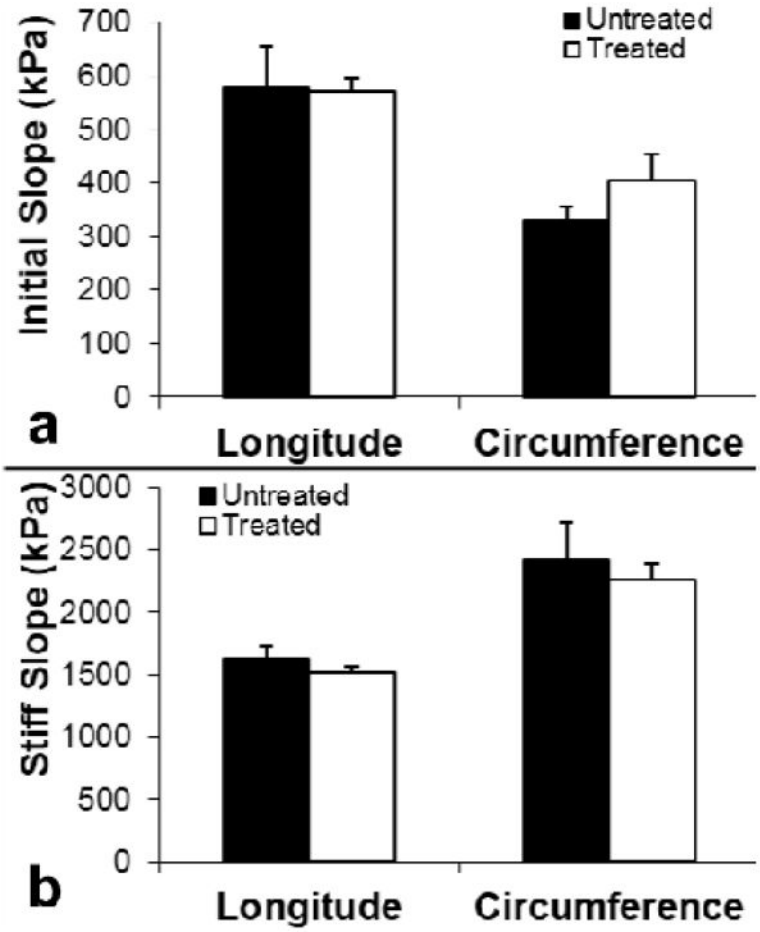

Fig. 4.

The (a) initial and (b) stiff slopes based on the stress-strain curves from equibiaxial tests of untreated aorta and after GAG removal treatment. There was no significant change in the slopes with GAG removal (n=6, p>0.1).

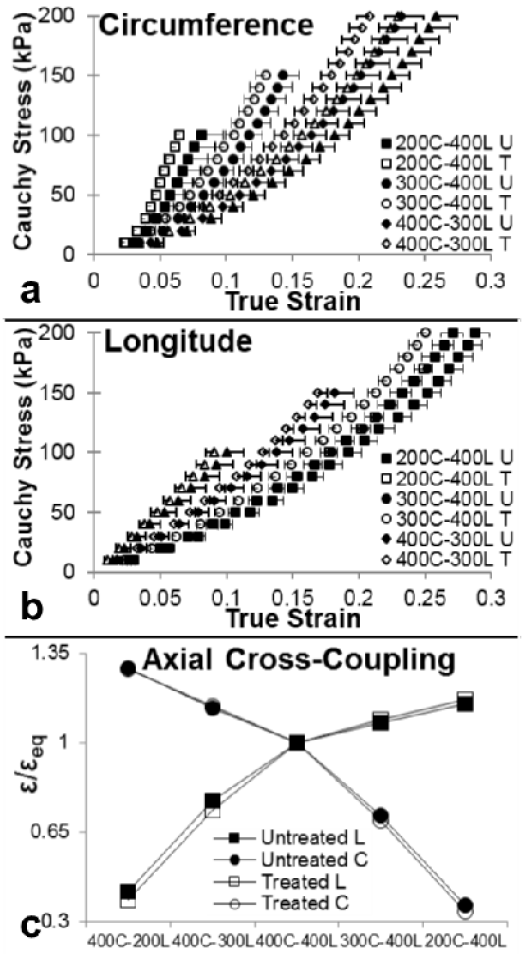

Fig. 5.

Averaged stress-strain curves from non-equibiaxial tensile tests (n=6) in the (a) circumferential, and (b) longitudinal directions before and after GAG removal. (c) Axial cross- coupling to examine the effect of GAG removal on mechanical coupling between material axes.

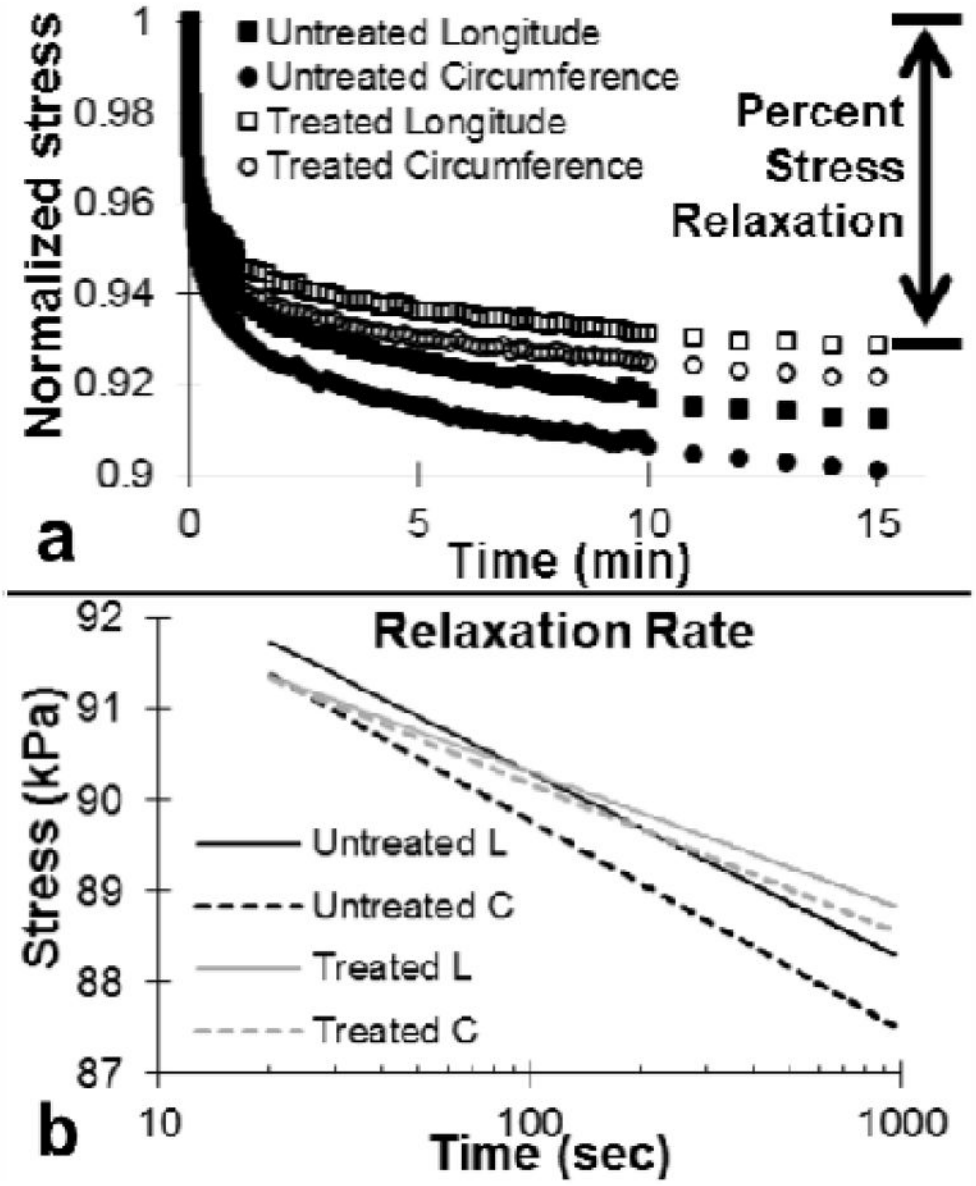

Fig. 6.

(a) Normalized stress relaxation results of aorta before and after GAG removal treatment. (b) The slope of stress vs. log of time gives the rate of relaxation in the longitudinal and circumferential directions, respectively (n=6).

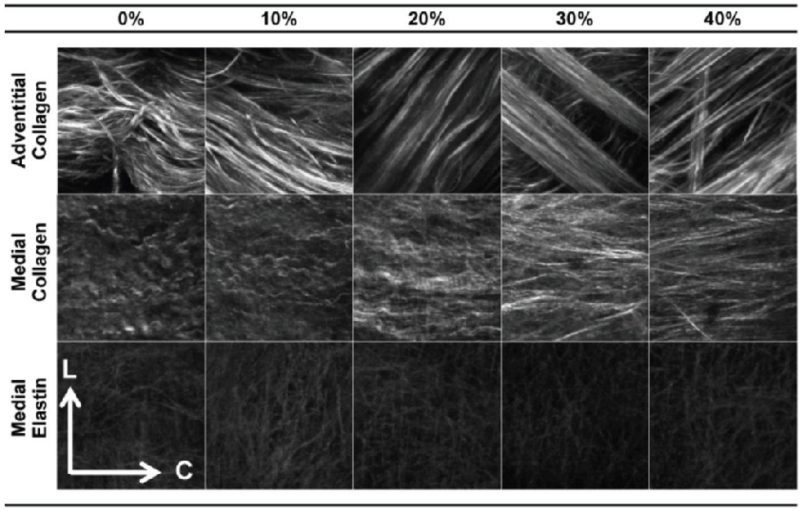

Fig. 7.

Fibers at different levels of equibiaxial stretch, where the numbers represent grip-to-grip strain for circumferential (C) and longitudinal (L) directions at 0° and ±90°, respectively. Images are 110μm × 110μm

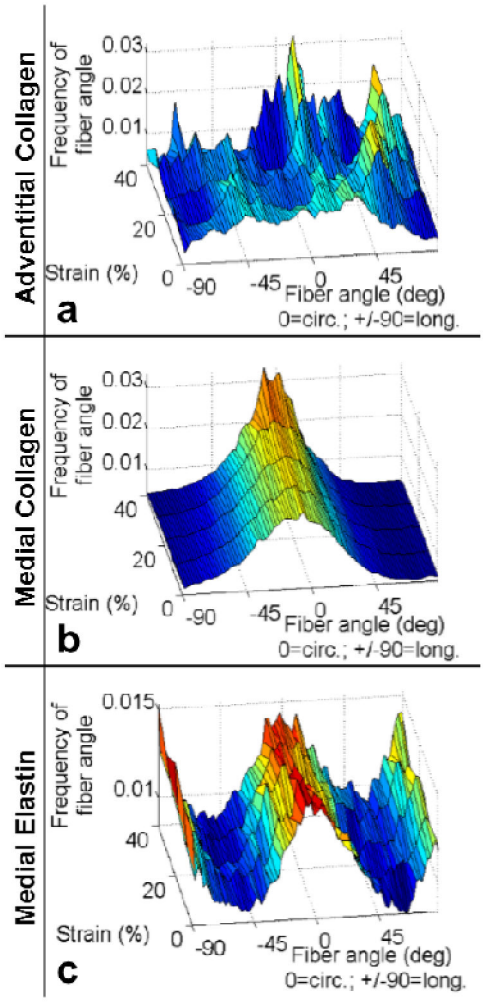

Fig. 8.

Fiber distributions of (a) adventitial collagen, (b) medial collagen, and (c) medial elastin during equibiaxial deformation of aorta tissue with GAGs removed.

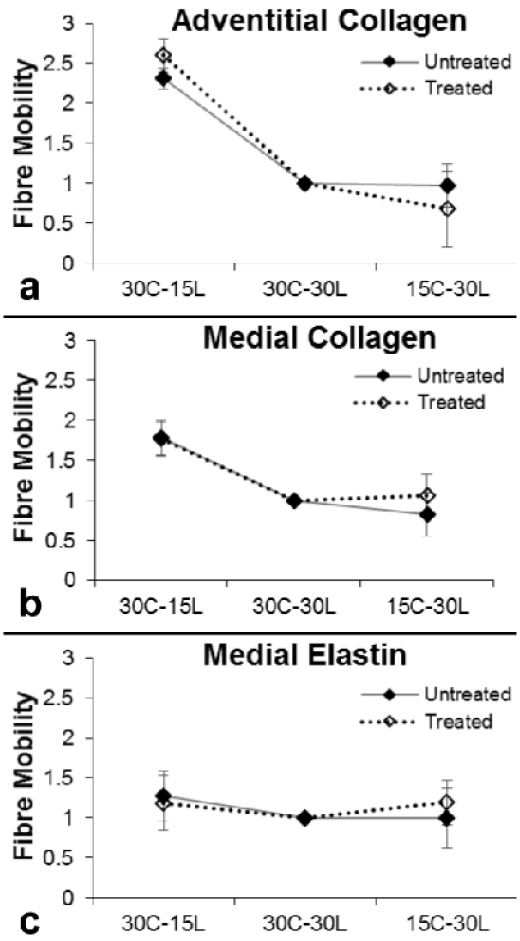

Fig. 9.

Fiber mobility of (a) adventitial collagen, (b) medial collagen, and (c) medial elastin. Both untreated and treated tissue show similar behavior, indicating no change to fiber mobility.

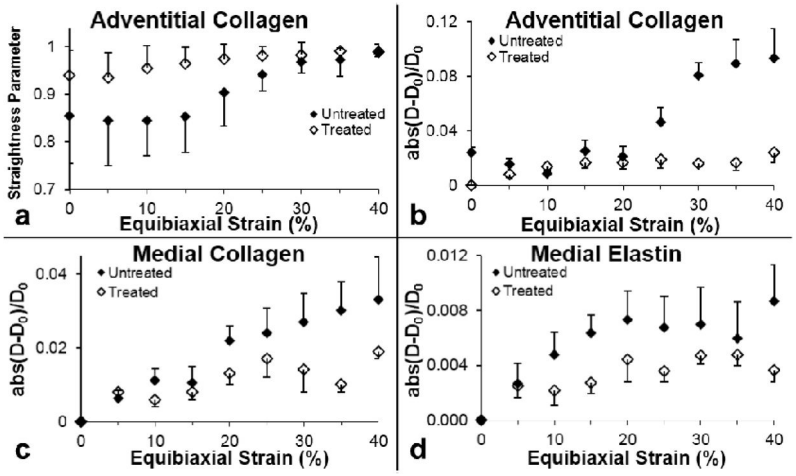

Fig. 10.

(a) Straightness parameter for adventitial collagen, and fractal analysis for (b) adventitial collagen, (c) medial collagen, and (d) medial elastin.